THE JOURNAL OF BIOLOGICAL CHEMISTRY VOL. 285, NO. 40, pp. 30523–30530, October 1, 2010

Hrs Controls Sorting of the Epithelial Na^+ Channel between Endosomal Degradation and Recycling Pathways*

Received for publication, June 2, 2010, and in revised form, July 30, 2010 Published, JBC Papers in Press, July 30, 2010, DOI 10.1074/jbc.M110.150755

Ruifeng Zhou[‡], Rajesh Kabra[‡], Diane R. Olson[‡], Robert C. Piper[§], and Peter M. Snyder[‡§1]

From the Departments of [‡]Internal Medicine and [§]Molecular Physiology and Biophysics, Roy J. and Lucille A. Carver College of Medicine, University of Iowa, Iowa City, Iowa 52242

Epithelial Na^+ absorption is regulated by Nedd4-2, an E3 ubiquitin ligase that reduces expression of the epithelial Na^+ channel (ENaC) at the cell surface. Defects in this regulation cause Liddle syndrome, an inherited form of hypertension. Previous work found that Nedd4-2 functions through two distinct effects on trafficking, enhancing both ENaC endocytosis and ENaC degradation in lysosomes. To investigate the mechanism by which Nedd4-2 targets ENaC to lysosomes, we tested the role of hepatocyte growth factor-regulated tyrosine kinase substrate (Hrs), a component of the endosomal sorting complexes required for transport (ESCRT)-0 complex. We found that α-, β-, and γENaC each interact with Hrs. These interactions were enhanced by Nedd4-2 and were dependent on the catalytic function of Nedd4-2 as well as its WW domains. Mutation of ENaC PY motifs, responsible for inherited hypertension (Liddle syndrome), decreased Hrs binding to ENaC. Moreover, binding of ENaC to Hrs was reduced by dexamethasone/serum- and glucocorticoid-inducible kinase and cAMP, which are signaling pathways that inhibit Nedd4-2. Nedd4-2 bound to Hrs and catalyzed Hrs ubiquitination but did not alter Hrs protein levels. Expression of a dominant negative Hrs lacking its ubiquitin-interacting motif (Hrs-ΔUIM) increased ENaC surface expression and current. This occurred through reduced degradation of the cell surface pool of proteolytically activated ENaC, which enhanced its recycling to the cell surface. In contrast, Hrs-ΔUIM had no effect on degradation of uncleaved inactive channels. The data support a model in which Nedd4-2 induces binding of ENaC to Hrs, which mediates the sorting decision between ENaC degradation and recycling.

The epithelial Na^+ channel ENaC[2] is composed of three homologous subunits (α, β, and γ) and functions in Na^+ transport across epithelia in the kidney collecting duct and connecting tubule, lung, and distal colon, where it plays a critical role in Na^+ homeostasis (reviewed in Refs. 1 and 2). Defects in ENaC regulation cause most of the identified genetic forms of hypertension. For example, mutations in β- and γENaC cause Liddle syndrome, an autosomal dominant form of hypertension (3). Conversely, loss of function mutations cause a salt-wasting disorder known as pseudohypoaldosteronism type 1 (3). In the lung, ENaC controls the composition and quantity of airway surface liquid, and defective ENaC regulation may contribute to lung disease in cystic fibrosis (4). Thus, understanding the mechanisms that regulate ENaC may provide new insights into the pathogenesis of hypertension, cystic fibrosis, and other diseases of Na^+ homeostasis.

Epithelial Na^+ absorption is regulated in large part by mechanisms that control ENaC expression at the apical membrane of epithelia. Here, the E3 ubiquitin ligase Nedd4-2 plays an important role (reviewed in Ref. 5). Nedd4-2 binds to ENaC channels located at the cell surface (6). This interaction occurs through binding of PY motifs located within the C termini of α-, β-, and γENaC to multiple WW domains in Nedd4-2 (6–8). Binding is critical for ENaC regulation. Disruption of binding by mutation of the PY motifs causes hypertension in Liddle syndrome (9–11). Binding is also important for the hormonal regulation of ENaC. Aldosterone and vasopressin activate signaling pathways that lead to Nedd4-2 phosphorylation by serum- and glucocorticoid-inducible kinase (SGK) and cAMP-dependent protein kinase (PKA), respectively (5). Phosphorylation reduces Nedd4-2 binding to ENaC, which enhances epithelial Na^+ transport (12–15).

Following binding, Nedd4-2 catalyzes mono- and polyubiquitination of each ENaC subunit (6), which reduces ENaC surface expression through two distinct mechanisms. First, Nedd4-2 increases the rate of ENaC endocytosis (16). This process involves epsin, which links ubiquitinated ENaC to the clathrin-based endocytic pathway (17). Second, once in endosomes, Nedd4-2 increases ENaC degradation in lysosomes, which reduces ENaC recycling back to the cell surface (16, 18).

A key unanswered question is what are the endosomal proteins that recognize ubiquitinated ENaC and direct it to the lysosomal degradation pathway? Proteins that comprise the endosomal sorting complexes required for transport (ESCRT)-0 complex are strong candidates. ESCRT-0 is a heterodimer of hepatocyte growth factor-regulated tyrosine kinase substrate (Hrs) and signal-transducing adaptor molecule (STAM) (reviewed in Refs. 20 and 21). In yeast, where many of the details of the pathway have been elucidated, the corresponding proteins are vacuolar protein sorting 27p (Vps27p) and Hbp, STAM, and EAST (Hse1p) (22, 23). The complex is localized to endosomes through the binding of a Fab1, YotB, Vacl, and EEA1 (FYVE) domain in Hrs to phosphatidylinositol

* This work was supported, in whole or in part, by National Institutes of Health Grant HL058812 (to P. M. S. and R. C. P.).

[1] To whom correspondence should be addressed: 371 EMRB, University of Iowa, Iowa City, IA 52242. E-mail: peter-snyder@uiowa.edu.

[2] The abbreviations used are: ENaC, epithelial Na^+ channel; FRT, Fischer rat thyroid; ESCRT, endosomal sorting complexes required for transport; UIM, ubiquitin-interacting motif; Hrs, hepatocyte growth factor-regulated tyrosine kinase substrate; STAM, signal-transducing adaptor molecule; SGK, serum- and glucocorticoid-inducible kinase; MTSET, [2-(trimethylammonium)ethyl]methanethiosulfonate bromide; Ni-NTA, nickel-nitrilotriacetic acid.

3-phosphate in the surface of endosomes (24). Both Hrs and STAM contain ubiquitin-interacting motifs (UIMs), which allow them to bind to ubiquitinated proteins (25, 26). In concert with additional ESCRT complexes, Hrs and STAM are thought to direct ubiquitinated membrane proteins into the endosomal lumen, forming multivesicular bodies that fuse with lysosomes to induce protein degradation. Consistent with this model, disruption of the Hrs-STAM complex or yeast homologues reduced lysosomal/vacuolar degradation of several cargo proteins, including the epithelial growth factor receptor (27), the G protein-coupled receptor CXCR4 (28), and the yeast α-factor receptor Ste3p (23, 29). Targeting to the endosomal lumen is dependent on the UIMs in Hrs/Vps27p and STAM/Hse1p (23, 29). Because the control of ENaC surface expression is critical for regulating epithelial Na^+ transport, we tested the role of Hrs in the sorting decision between ENaC degradation and recycling.

EXPERIMENTAL PROCEDURES

cDNA Constructs—Human α-, β-, and γENaC in pMT3 were cloned as described previously (30, 31). The following ENaC cDNAs were used: α-FLAG, β-FLAG, and γ-FLAG (each inserted at the C terminus) (6, 11); α_{Y644A}, β_{Y620A}, and γ_{Y627A} (9); $\alpha_{Cl\text{-}1}$ (R177A, R178A) and $\alpha_{Cl\text{-}2}$ (R175A, R177A, R178A, R181A, R190A, R192A, R201A, R204A) (16); and γ_{Cl} (R135A, R137A, R138A, R178W, R180A, K181A) and $\gamma_{Cl\text{-}G536C}$. Additional cDNAs used were human Nedd4-2 in pMT3 (12), Nedd4-2_{WW} (V210W, H212G, V367W, H369G, I440W, H442G, I492W, H494G) (6), Nedd4-2_{C821A} (6), Nedd4-$2_{S/T\text{-}A}$ (S221A, T246A, S327A) (12), human SGK in pMT3 (12), mouse Hrs with C-terminal HA epitope in pcDNA3 and Hrs-ΔUIM (S270A, Q271A, S272A, E273A) (27), and ubiquitin-His (in pMT123) (6).

Cell Culture and Transfection—HEK 293T and COS-7 cells were cultured in Dulbecco's modified Eagle's medium. The cells were transfected with cDNAs encoding Hrs-HA, $\alpha\beta\gamma$ENaC (one subunit containing a C-terminal FLAG epitope), and Nedd4-2 using Lipofectamine 2000 (Invitrogen). In some experiments, cells were cotransfected with SGK (see Fig. 3, *C* and *D*) or ubiquitin-His (see Figs. 4*B* and 7*D*). The total cDNA concentration was held constant using GFP cDNA (cDNA concentrations are reported in the legends for Figs. 1–8). Following transfection, 10 μM amiloride was added to the culture medium. In Fig. 3, *A* and *B*, cells were incubated in serum-free medium with or without dexamethasone (100 nM) for 4 h, and in Fig. 3, *E* and *F*, cells were treated with 200 μM 8-(4-chlorophenylthio)-cAMP sodium (Sigma), 100 μM 3-isobutyl-1-methylxanthine (Sigma), and 10 μM forskolin (Sigma) for 2 h prior to harvest. Cells were harvested 48 h after transfection.

Fischer rat thyroid (FRT) cells were cultured on permeable filter supports (Millicell PCF, 0.4-μm pore size, 12-mm diameter) in F-12 Coon's medium (Sigma) with 5% fetal calf serum (Sigma), 100 units/ml penicillin, and 100 μg/ml streptomycin at 37 °C, as described previously (32). 1 day after seeding, cells were cotransfected with $\alpha\beta\gamma$ENaC (wild-type or mutant) and human Nedd4-2, with or without Hrs-ΔUIM (total cDNA was held constant with GFP cDNA) using TFX 50 (Promega). 1 h after transfection, 10 μM amiloride was added to the apical medium, and currents were recorded 48 h after transfection.

Coimmunoprecipitation—48 h after transfection, HEK 293T cells were lysed in 150 mM NaCl, 50 mM Tris (pH 7.4), 0.5% Nonidet P-40, and protease inhibitor mixture (Sigma). 500 μg of protein was immunoprecipitated with anti-FLAG M2 affinity gel (Sigma), anti-HA antibody (1:300, Sigma), or anti-WW1 antibody (1:50 (8)) with immobilized protein A (Pierce) or Ni-NTA beads (Qiagen). After extensive washing, the immunoprecipitated proteins were eluted in SDS-PAGE sample loading buffer (100 mM dithiothreitol, 20% glycerol, 100 mM Tris-Cl, pH 6.8, and 4% SDS) at 95 °C for 5 min and then separated by SDS-PAGE. Cell lysates (10 μg) were also separated by SDS-PAGE. Proteins were detected by immunoblot with anti-FLAG M2 monoclonal antibody-peroxidase conjugate (Sigma) at 1: 5000 dilution or anti-HA antibody (1:2000) and enhanced chemiluminescence (ECL Plus, GE Healthcare) and quantitated by densitometry using the ImageJ software.

Cell Surface Biotinylation—Transfected HEK 293T cells were washed with ice-cold PBS-CM (PBS with 1 mM $CaCl_2$ and $MgCl_2$) three times on ice, labeled with 0.5 mg/ml Sulfo-NHS-biotin (Pierce) in PBS-CM for 30 min on ice, and quenched by incubating with 100 mM glycine in PBS-CM for 10 min. After washing three times with PBS-CM, cells were lysed in 0.4% sodium deoxycholate, 1% Nonidet P-40, 63 mM EDTA, 50 mM Tris-HCl, pH 8, and protease inhibitor mixture. Biotin-labeled cell surface proteins were isolated by incubating cell lysate (200 μg) with immobilized NeutrAvidin beads (Pierce) for 12 h at 4 °C, detected by immunoblot (anti-FLAG M2 monoclonal antibody-peroxidase conjugate), and quantitated by densitometry using the ImageJ software.

To measure the rate of ENaC endocytosis, HEK 293T cells transfected with $\alpha_{Cl\text{-}2}$-FLAG, β- and γENaC, Nedd4-2, and Hrs-ΔUIM or GFP were incubated with trypsin (5 μg/ml) for 5 min at 37 °C, as described previously (16). The cells were washed three times with PBS-CM to remove trypsin, incubated at 37 °C for times between 0 and 30 min to allow endocytosis of cleaved channels, and then placed on ice. Cleaved channels remaining at the cell surface were labeled with Sulfo-NHS-biotin, isolated with NeutrAvidin beads, detected by immunoblot, and quantitated by densitometry using ImageJ software.

To measure the rate of degradation of the cell surface fraction of ENaC, HEK 293T cells were biotinylated with Sulfo-NHS-biotin and then incubated at 37 °C for 0–120 min prior to lysis. Following lysis, remaining biotinylated ENaC was isolated with NeutrAvidin beads, detected by immunoblot, and quantitated by densitometry using ImageJ software (6).

Electrophysiology—Short circuit current was measured using modified Ussing chambers (Warner Instrument Corp.) in transfected FRT cells (12). The apical and basolateral surfaces were bathed in 135 mM NaCl, 1.2 mM $CaCl_2$, 1.2 mM $MgCl_2$, 2.4 mM K_2HPO_4, 0.6 mM KH_2PO_4, 10 mM HEPES (pH 7.4) at 37 °C. ENaC current was determined by subtracting current before and after the addition of 10 μM amiloride to the apical surface.

To quantitate ENaC endocytosis, FRT cells were transfected with $\alpha_{Cl\text{-}1}$, β- and γ_{Cl} ENaC, and Hrs-ΔUIM or GFP, as described previously (16). Electrically silent ENaC channels at the cell surface were activated by proteolytic cleavage using

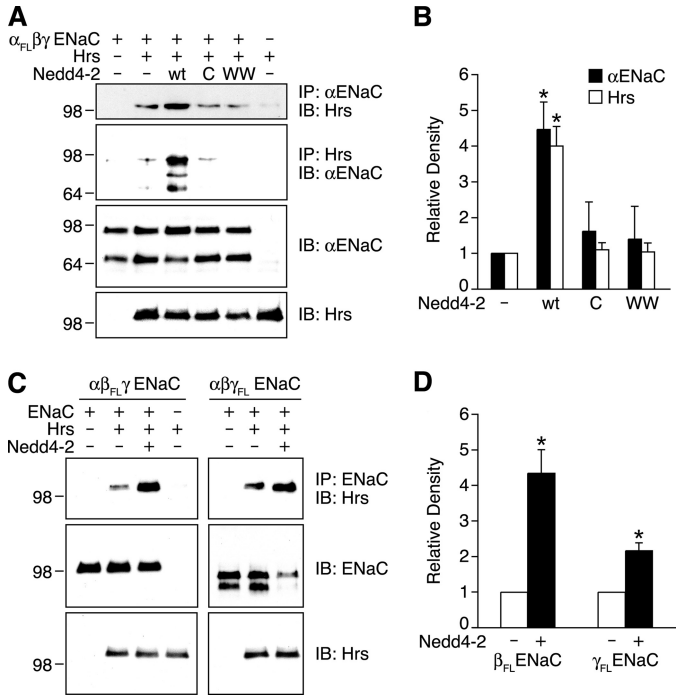

FIGURE 1. **ENaC interacts with Hrs.** *A* and *B*, coimmunoprecipitation of αENaC and Hrs in HEK 293T cells transfected with α-FLAG, β-, and γENaC (1.5 μg each), with or without Hrs-HA (0.5 μg) and Nedd4-2 (*wt*, wild type; *C*, C821A; *WW*, WW domain mutant) (0.5 μg). Total cDNA was held constant using GFP cDNA. *A*, representative immunoblots. In the *top two panels*, cell lysates were immunoprecipitated (*IP*) and immunoblotted (*IB*) as indicated with antibodies against αENaC (anti-FLAG) or Hrs (anti-HA). The *bottom two panels* show immunoblots of cell lysates. *B*, quantitation of αENaC that coprecipitated with Hrs (*black bars*) and of Hrs that coprecipitated with ENaC (*white bars*), relative to the group expressing ENaC and Hrs without Nedd4-2. Data are mean ± S.E. ($n = 3–8$, *, $p < 0.03$). *C* and *D*, coimmunoprecipitation of β-FLAG or γ-FLAG (coexpressed with the other two untagged ENaC subunits) and Hrs in HEK 293T cells using the methods described in *panel A*. *C* shows representative immunoblots, and *D* shows quantitation of Hrs coprecipitated with ENaC. Data are mean ± S.E. ($n = 4–5$, *, $p < 0.003$).

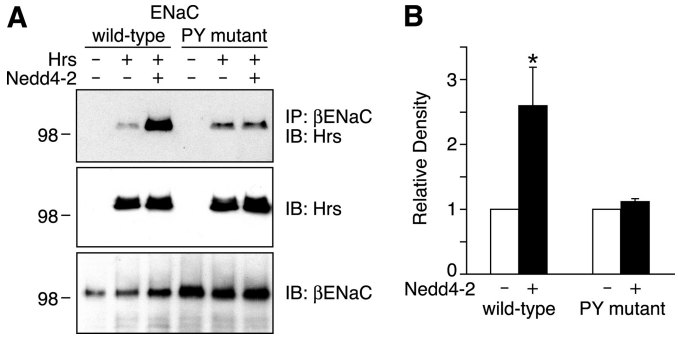

FIGURE 2. **ENaC PY motifs are required for Nedd4-2 to enhance ENaC-Hrs interaction.** *A* and *B*, coimmunoprecipitation of βENaC and Hrs in HEK 293T cells transfected with α-, β-FLAG, and γENaC (wild-type or $\alpha_{Y644A}\beta_{Y620A}\gamma_{Y627A}$, 1.5 μg each), with or without Hrs-HA (0.5 μg) and Nedd4-2 (0.5 μg). *A*, representative immunoblots. In the *top panel*, βENaC was immunoprecipitated with anti-FLAG antibody followed by immunoblot for Hrs with anti-HA antibody. The *bottom two panels* show immunoblots of cell lysates to detect Hrs (anti-HA) or βENaC (anti-FLAG), as indicated. *B*, quantitation of Hrs that coprecipitated with βENaC (relative to the group expressing ENaC and Hrs without Nedd4-2). Data are mean ± S.E. ($n = 4$, *, $p < 0.04$).

trypsin (10 μg/μl), which was added to the apical membrane for 10 min and then removed by vigorous washes with ~12 times the volume of the apical chamber. The time-dependent decline in ENaC current was measured every 5 min by the addition of amiloride (10 μM) to the apical membrane followed by washout of amiloride.

To quantitate ENaC recycling, FRT cells were transfected with $\alpha_{Cl\text{-}1}$, β- and $\gamma_{Cl\text{-}G536C}$ ENaC, and Hrs-ΔUIM or GFP. The apical membrane was incubated for 30 min with trypsin (10 μg/μl) at 37 °C to generate a pool of active ENaC that could undergo endocytosis. ENaC remaining at the cell surface was irreversibly blocked with 1 mM [2-(trimethylammonium)ethyl]-methanethiosulfonate bromide (MTSET, Toronto Research Chemicals). After removal of MTSET, we monitored the rate of increase in benzamil-sensitive current (100 μM) as an assay of the return of active channels to the cell surface.

Statistics—Data are reported as mean ± S.E. Significance was determined by Student's *t* test ($p < 0.05$).

RESULTS

Interaction of ENaC with Hrs—To investigate the role of Hrs in targeting ENaC for degradation, we first tested whether Hrs binds to ENaC. In Fig. 1*A*, we cotransfected HEK 293 cells with α-FLAG, β- and γENaC and Hrs-HA. The immunoblots in the *bottom two panels* show that αENaC and Hrs proteins were expressed (the two αENaC bands correspond to the full-length and proteolytically cleaved forms). The *top two panels* show coimmunoprecipitation experiments. Following immunoprecipitation of αENaC, we detected Hrs by immunoblot only in cells in which ENaC and Hrs were coexpressed but not in cells expressing ENaC or Hrs alone (Fig. 1*A*, *top panel*). Likewise, when we immunoprecipitated Hrs, we detected a faint αENaC band (Fig. 1*A*, *second panel*). Together, the data indicate that Hrs interacts with αENaC.

Nedd4-2 catalyzes ENaC ubiquitination, which increases ENaC degradation in lysosomes (6, 18). We therefore tested the effect of Nedd4-2 on the ENaC-Hrs interaction. When cotransfected in HEK 293 cells, we found that Nedd4-2 increased binding of Hrs to αENaC but had no significant effect on total cellular αENaC or Hrs protein levels (Fig. 1*A*). Fig. 1*B* shows quantitation of αENaC that coprecipitated with Hrs and Hrs that coprecipitated with αENaC, as indicated. Mutation of the catalytic HECT domain (C821A) abolished the effect of Nedd4-2 (Fig. 1, *A* and *B*), indicating that ubiquitination is required for Nedd4-2 to modulate αENaC-Hrs binding. The effect of Nedd4-2 on binding was also abolished by mutation of its WW domains (Fig. 1, *A* and *B*), which mediate Nedd4-2 binding to ENaC.

In Fig. 1*C*, we asked whether Hrs would also bind to β- and γENaC. Similar to αENaC, we found that Hrs coprecipitated with both βENaC and γENaC. Moreover, Nedd4-2 increased Hrs binding to β- and γENaC (Fig. 1, *C* and *D*). Thus, Hrs interacts with all three ENaC subunits in a manner that is facilitated by Nedd4-2.

Liddle syndrome is caused by mutations that disrupt Nedd4-2 binding to ENaC PY motifs (9–11). In contrast to wild-type ENaC, Nedd4-2 failed to enhance the binding of βENaC to Hrs when the ENaC PY motifs were mutated (Fig. 2, *A* and *B*). Together with our similar finding when we mutated the Nedd4-2 WW domains (Fig. 1, *A* and *B*), the data suggest

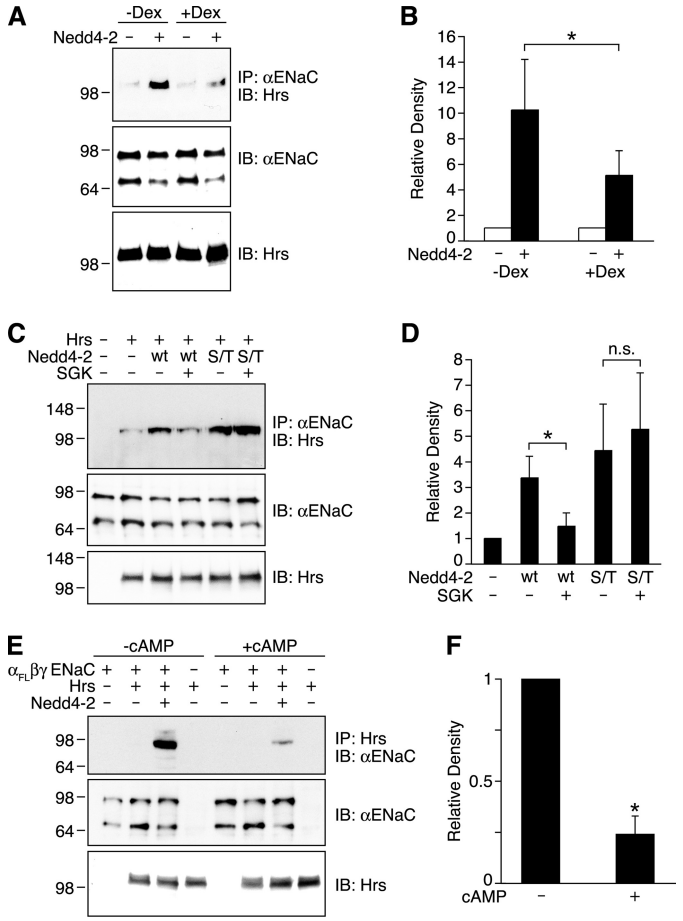

FIGURE 3. **Phosphorylation regulates ENaC binding to Hrs.** *A–F*, coimmunoprecipitation of αENaC and Hrs in HEK 293T cells transfected with α-FLAG, β-, and γENaC (1.5 μg each), with or without Hrs-HA (0.5 μg) and Nedd4-2 (*wt*, wild type; *S/T*, phosphorylation mutant) (0.5 μg). Total cDNA was held constant using GFP cDNA. Immunoprecipitation (*IP*) and immunoblot (*IB*) utilized anti-FLAG (αENaC) and anti-HA (Hrs) antibodies, as indicated. *A*, cells were incubated in serum-free medium with or without dexamethasone (*Dex*, 100 nM) for 4 h prior to harvest. Data for coprecipitation are quantitated in *B* (mean ± S.E., $n = 3$, *, $p < 0.03$). *C*, cells were cotransfected with or without SGK (1 μg), as indicated. For groups expressing ENaC and Hrs, data for coprecipitation are quantitated in *D* (mean ± S.E., $n = 4$, *, $p < 0.04$, *n.s.* indicates that the *p* value was not statistically significant). *E*, cells were treated with or without cAMP agonists (200 μM 8-(4-chlorophenylthio)-cAMP sodium, 100 μM 3-isobutyl-1-methylxanthine, 10 μM forskolin) for 2 h, as indicated. For groups expressing ENaC with Hrs and Nedd4-2, coimmunoprecipitation data are quantitated in *F* (mean ± S.E., $n = 4$, *, $p < 0.002$).

that the interaction between Nedd4-2 and ENaC is required for Nedd4-2 to modulate ENaC binding to Hrs.

Phosphorylation Regulates ENaC Binding to Hrs—ENaC trafficking is regulated by glucocorticoids and mineralocorticoids, in part through phosphorylation of Nedd4-2 (5). In Fig. 3, *A* and *B*, we tested the effect of the glucocorticoid dexamethasone on the interaction between ENaC and Hrs. Cells were cultured with or without dexamethasone for 4 h prior to lysis. In the absence of dexamethasone, Nedd4-2 increased αENaC binding to Hrs. In contrast, when cells were treated with dexamethasone, Nedd4-2 produced a smaller increase in binding (but had no effect on αENaC or Hrs protein levels).

Dexamethasone induces transcription of SGK (33, 34), which phosphorylates Nedd4-2 on three Ser/Thr residues, reducing its binding to ENaC (12–14). We therefore tested whether SGK would regulate the effect of Nedd4-2 on ENaC binding to Hrs.

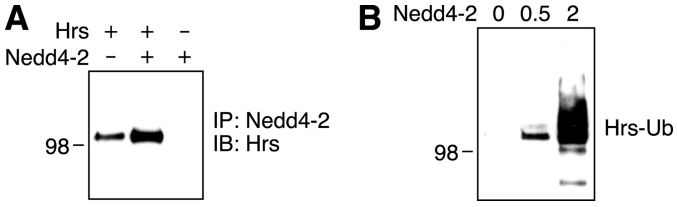

FIGURE 4. **Nedd4-2 binds to and ubiquitinates Hrs.** *A*, coimmunoprecipitation of Hrs and Nedd4-2 in COS 7 cells transfected with or without Hrs-HA (2 μg) and Nedd4-2 (2 μg). Nedd4-2 was immunoprecipitated (*IP*) (anti-WW1 antibody) followed by immunoblot (*IB*) for Hrs (anti-HA antibody). *B*, ubiquitinated Hrs in HEK 293T cells transfected with Hrs-HA (2 μg), ubiquitin-His (1 μg), and the indicated amount of Nedd4-2 (0–2 μg). Ubiquitinated Hrs (*Hrs-Ub*) was pulled down with Ni-NTA beads and detected by immunoblot (anti-HA antibody). The immunoblots are representative of three experiments.

In cells transfected with SGK, Nedd4-2 failed to increase αENaC-Hrs binding, in contrast to cells not transfected with SGK (Fig. 3, *C* and *D*). This effect of SGK was dependent on its ability to phosphorylate Nedd4-2; mutation of the three SGK phosphorylation sites in Nedd4-2 (S/T) abolished the effect of SGK on ENaC-Hrs binding (Fig. 3, *C* and *D*). Together, the data indicate that SGK regulates the interaction between ENaC and Hrs through its phosphorylation of Nedd4-2.

Another Ser/Thr kinase, PKA, also phosphorylates Nedd4-2 and reduces its binding to ENaC (14). PKA is a downstream mediator of vasopressin, a hormone important in the regulation of epithelial Na^+ and water transport (35). In Fig. 3, *E* and *F*, we modulated PKA activity by incubating cells for 2 h with or without cAMP agonists. In cells cotransfected with Nedd4-2, cAMP agonists reduced binding of αENaC to Hrs, similar to the effect of SGK. Thus, ENaC binding to Hrs can be modulated by at least two signaling pathways.

Interaction of Hrs with Nedd4-2—To further investigate the mechanisms by which Nedd4-2 regulates ENaC binding to Hrs, we asked whether Nedd4-2 and Hrs interact with one another. In Fig. 4*A*, we immunoprecipitated Nedd4-2 (anti-WW domain 1) and detected coprecipitated Hrs by immunoblot (anti-HA). We detected coprecipitated Hrs in cells cotransfected with Hrs and Nedd4-2. We also detected a small amount of coprecipitated Hrs in cells transfected with Hrs alone (Fig. 4*A*), likely through its binding to endogenous Nedd4-2. These findings support the conclusion that Nedd4-2 and Hrs form a complex.

Because Nedd4-2 is an E3 ubiquitin ligase, we tested the possibility that Nedd4-2 might catalyze Hrs ubiquitination. In Fig. 4*B*, we found that Nedd4-2 induced Hrs ubiquitination. However, ubiquitination did not induce Hrs degradation; in Figs. 1–3, Nedd4-2 failed to significantly reduce Hrs protein levels.

Effect of Hrs on ENaC Surface Expression—To test the role of Hrs in controlling ENaC surface expression, we overexpressed a dominant negative Hrs that lacks its ubiquitin-interacting motif (Hrs-ΔUIM). Previous work found that this construct disrupted the endosomal sorting of the epidermal growth factor receptor (36), similar to work with the yeast homologue Vps27p (23, 29). In Fig. 5*A*, we cotransfected α-FLAG and β- and γENaC in HEK 293 cells with or without Nedd4-2 and Hrs-ΔUIM and then detected the biotinylated cell surface fraction of αENaC by immunoblot. Nedd4-2 dramatically reduced αENaC surface expression but had minimal effect on αENaC in

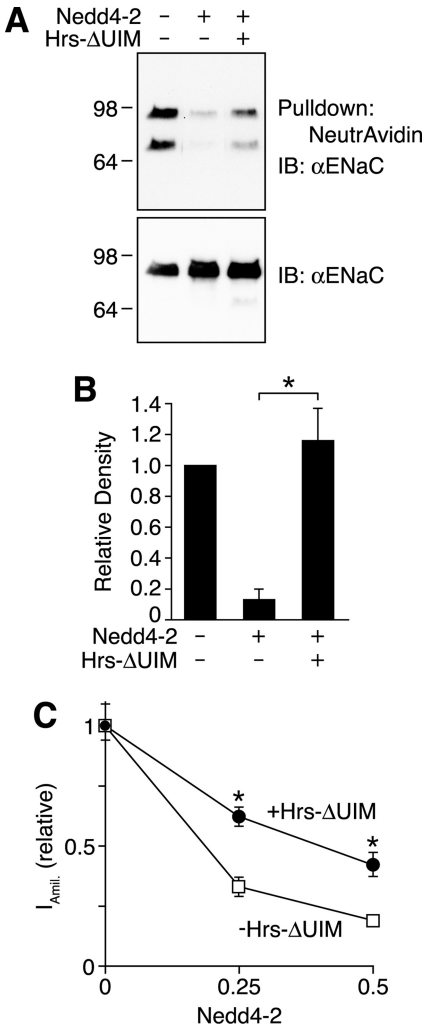

FIGURE 5. **Effect of Hrs on ENaC surface expression.** *A*, immunoblots (*IB*) (anti-FLAG) of biotinylated (*top panel*) and total (*bottom panel*) αENaC in HEK 293T cells transfected with α-FLAG, β-, and γENaC (1 μg each), with or without Nedd4-2 (0.06 μg) and Hrs-ΔUIM (4 μg). Total cDNA was held constant using GFP cDNA. Irrelevant lanes were removed from the images. αENaC surface expression is quantitated in *B*, relative to the group without Nedd4-2 and Hrs-ΔUIM (mean ± S.E., $n = 5$, *, $p < 0.003$). *C*, amiloride-sensitive short circuit current (relative to the group without Nedd4-2) in FRT cells transfected with α-, β-, and γENaC, with or without Nedd4-2 and Hrs-ΔUIM (cDNA ratio 1:0–0.5:4; total cDNA was held constant using GFP cDNA). Data are mean ± S.E. ($n = 10–11$, *, $p < 0.001$).

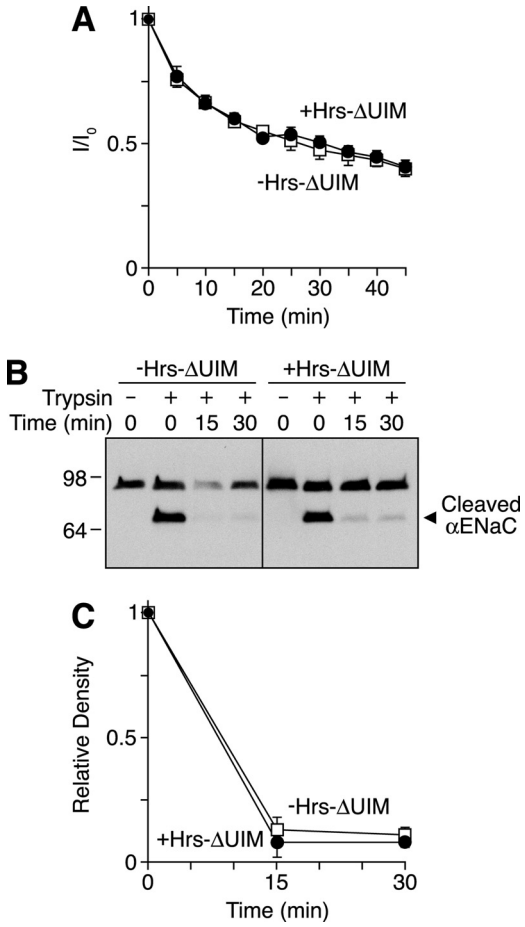

FIGURE 6. **Effect of Hrs on ENaC endocytosis.** *A*, trypsin-activated amiloride-sensitive short circuit current *versus* time after trypsin removal in FRT cells transfected with α_{Cl-1}, β-, and γ_{Cl}ENaC (0.25 μg each) and Hrs-ΔUIM (*black circles*) or empty vector (*white squares*) (0.25 μg). Data are mean ± S.E. ($n = 8$). *B*, immunoblot (anti-FLAG) of biotinylated αENaC in HEK 293T cells transfected with α_{Cl-2}-FLAG, β-, and γENaC (1 μg each), Nedd4-2 (0.06 μg), and with or without Hrs-ΔUIM (4 μg). The cells were incubated with or without trypsin (5 μg/ml for 5 min), incubated at 37 °C for 0–30 min, and then biotinylated. The cleaved αENaC bands are quantitated in *C*, relative to 0 min (mean ± S.E., $n = 3$).

the total cellular pool, which primarily reflects ENaC in the biosynthetic pathway (6). Hrs-ΔUIM increased αENaC at the cell surface, reversing the effect of Nedd4-2 (Fig. 5*A* and quantitated in Fig. 5*B*).

To examine the functional consequence of this change in ENaC surface expression, we measured short circuit current in Fischer rat thyroid epithelia transfected with ENaC and Nedd4-2 with or without Hrs-ΔUIM. In the absence of Hrs-ΔUIM, Nedd4-2 inhibited amiloride-sensitive ENaC current in a dose-dependent manner (Fig. 5*C*). Hrs-ΔUIM reduced ENaC inhibition by Nedd4-2, shifting the dose-response relationship to the right. Thus, the functional and biochemical data indicate that the Hrs UIM is required for Nedd4-2 to regulate ENaC trafficking.

Effect of Hrs on ENaC Trafficking—Nedd4-2 regulates ENaC trafficking at two different steps in the endocytic pathway: endocytosis and lysosomal targeting (6, 16). To identify the step at which Hrs modulates Nedd4-2 function, we first asked whether Hrs-ΔUIM would alter ENaC endocytosis, using functional and biochemical approaches we previously described (16). In Fig. 6*A*, we used trypsin to acutely activate a furin-resistant (inactive) mutant ENaC expressed with Nedd4-2 in FRT epithelia. After removal of trypsin, we measured the rate of decay in amiloride-sensitive current as a measure of ENaC endocytosis. Current decay was rapid over the first 15–20 min and was identical in the presence or absence of Hrs-ΔUIM. As a biochemical correlate of this strategy, we measured the rate of disappearance of trypsin-cleaved furin-resistant channels from the cell surface using a biotinylation assay (Fig. 6*B*, and quantitated in Fig. 6*C*). Incubation of cells with trypsin for 5 min generated a pool of proteolytically cleaved α subunits, which were mostly removed over 15 min. Similar to the electrophysiological data, Hrs-ΔUIM did not alter the rate of disappearance of cleaved αENaC from the cell surface. Together, the data indicate that Hrs does not modulate ENaC endocytosis.

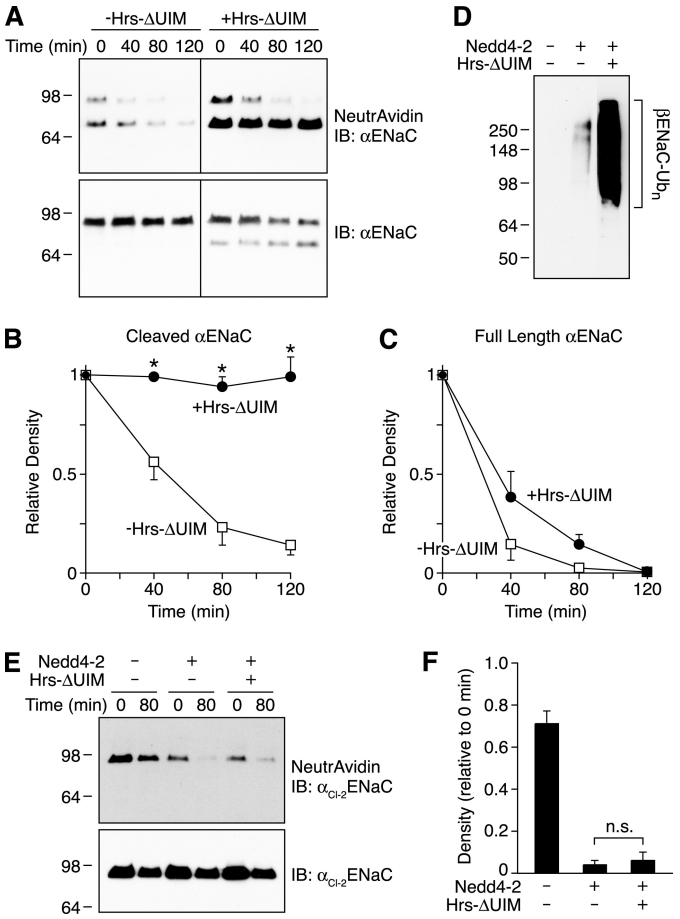

FIGURE 7. **Effect of Hrs on degradation of cell surface ENaC.** *A*, immunoblots (*IB*) (anti-FLAG) of biotinylated (*top panel*) and total (*bottom panel*) αENaC in HEK 293T cells transfected with α-FLAG, β-, and γENaC (1 μg each) with Nedd4-2 (0.06 μg) and with or without Hrs-ΔUIM (4 μg). Cell surface proteins were pulse-labeled with biotin, and then the cells were incubated at 37 °C for 0–120 min. Biotinylated αENaC at each time point was quantitated (relative to 0 min) in *B* (cleaved αENaC) and *C* (full-length αENaC). Data are mean ± S.E. ($n = 3$–4, *, $p < 0.02$). *D*, immunoblot of ubiquitinated βENaC (*βENaC-Ub*) in HEK 293T cells transfected with α-, β-FLAG, and γENaC (1 μg each), ubiquitin-His (1 μg), with or without Nedd4-2 (0.06 μg) and Hrs-ΔUIM (3 μg). The cells were incubated with 10 μM *N*-acetyl-Leu-Leu-norleucinal for 2 h prior to lysis. Ubiquitinated proteins were isolated with Ni-NTA beads followed by immunoblot for βENaC with anti-FLAG. Irrelevant lanes were removed from the image. *E*, immunoblots (anti-FLAG) of biotinylated (*top panel*) and total (*bottom panel*) αENaC in HEK 293T cells transfected with $\alpha_{Cl\text{-}2}$-FLAG, β-, and γENaC (1 μg each) with or without Nedd4-2 (0.06 μg) and Hrs-ΔUIM (4 μg). Cell surface proteins were pulse-labeled with biotin, and then the cells were incubated at 37 °C for 0 or 80 min. Biotinylated αENaC at 80 min was quantitated (relative to 0 min) in *F*. Data are mean ± S.E. ($n = 3$, *n.s.* indicates that the *p* value was not statistically significant).

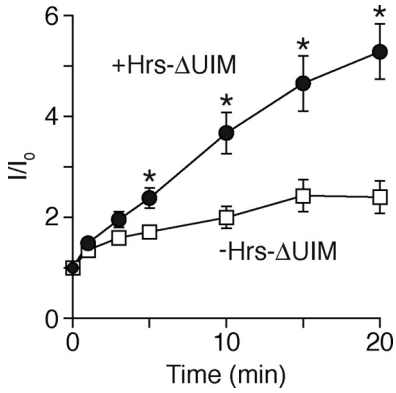

FIGURE 8. **Effect of Hrs on ENaC recycling.** Plot of recovery of benzamil-sensitive short circuit current *versus* time after MTSET removal in FRT cells transfected with $\alpha_{Cl\text{-}1}$, β-, and $\gamma_{Cl\text{-}G536C}$ ENaC (0.25 μg each) and Hrs-ΔUIM or empty vector (0.25 μg). The channels were activated by trypsin (10 μg/ml for 30 min), and then active channels remaining at the cell surface were irreversibly blocked with MTSET (1 mM). Data are mean ± S.E. ($n = 11$–12, *, $p <$ 0.02).

Once ENaC has reached the endosome, it can undergo degradation in lysosomes, or alternatively, recycle back to the cell surface to participate in Na^+ uptake. To test whether Hrs plays a role in this sorting decision, we biotinylated ENaC at the cell surface and then measured the rate of degradation of biotinylated αENaC. When coexpressed with Nedd4-2, the majority of αENaC was degraded at 80 min, consistent with our previous work (6, 16). Hrs-ΔUIM abolished degradation of the cleaved (active) αENaC band (Fig. 7, *A* and *B*). This resulted in an accumulation of ubiquitinated ENaC (Fig. 7*D*).

In contrast to its effect on the cleaved form of αENaC, Hrs-ΔUIM did not prevent the disappearance of the full-length (inactive) form (Fig. 7*C*). This disappearance reflects two processes: degradation and proteolytic conversion to the cleaved form. We tested the possibility that Hrs selectively controls degradation of cleaved channels using the furin-resistant αENaC mutant that does not undergo cleavage. In Fig. 7, *E* and *F*, we biotinylated the cell surface fraction of channels and then detected biotinylated channels before or after an 80-min incubation at 37 °C. Nedd4-2 increased degradation of the uncleaved α subunit, but Hrs-ΔUIM did not prevent its degradation. Thus, Hrs functions in selectively targeting proteolytically cleaved ENaC to lysosomes for degradation.

By targeting ENaC for degradation, Hrs might alter the size of the ENaC pool available for recycling back to the cell surface. To test this possibility, we used an electrophysiological approach to quantitate the rate of ENaC recycling. Using a furin-resistant inactive ENaC mutant as a backbone, we introduced a cysteine into the channel pore (γ_{G536C}). In previous work, we found that covalent modification of this cysteine irreversibly blocks the channel (37). We activated channels at the cell surface with trypsin and then incubated the cells at 37 °C for 30 min to allow some of the channels to undergo endocytosis. We then irreversibly blocked channels remaining at the cell surface with MTSET and (following washout of MTSET and trypsin) quantitated the rate of current recovery as a measure of recycling of the trypsin-cleaved channels. We found that Hrs-ΔUIM increased ENaC recycling, as reflected by the enhanced rate of current recovery (Fig. 8).

DISCUSSION

The sorting decision between ENaC degradation in lysosomes and ENaC recycling is a critical step in the regulation of epithelial Na^+ transport. Signals that increase degradation (*e.g.* Nedd4-2) reduce Na^+ transport, whereas signals that increase recycling (*e.g.* cAMP) increase Na^+ transport. In this work, we identified an important role for Hrs in this trafficking decision. We found that ENaC bound to Hrs, an interaction that was augmented by the E3 ubiquitin ligase Nedd4-2. Importantly, disruption of Hrs activity reduced degradation of the cell surface pool of ENaC and enhanced ENaC recycling to the cell surface. Together with previous work, these findings suggest a

model in which Nedd4-2 induces binding of ENaC to Hrs in endosomes, which in turn sorts ENaC to lysosomes for degradation.

There are three potential mechanisms by which Nedd4-2 might increase ENaC binding to Hrs. First, previous work indicates that Nedd4-2 causes the redistribution of ENaC from the cell surface to endosomes (18), the site of localization of Hrs. This colocalization within a common compartment would increase the amount of ENaC available to bind to Hrs. Second, Nedd4-2 catalyzes ENaC ubiquitination (6), which would mediate binding through an interaction with the Hrs ubiquitin-interacting motif. Third, Nedd4-2 could function as an adaptor to strengthen the interaction between ENaC and Hrs. Consistent with this possibility, we found that Nedd4-2 bound to Hrs. In this regard, ubiquitination of ENaC alone may not be the only feature that induces its association with Hrs. In addition to Nedd4-2, other HECT-type E3 ligases such as AIP4 and the yeast Rsp5 have been shown to interact with a wide variety of adaptors, some of which associate with ESCRT-0 (38–41). Thus, a convergence of several mechanisms including multiple protein-protein interactions is likely to drive the ENaC-Hrs association we see here.

ENaC gating is regulated in part by proteolytic cleavage of its extracellular domains, which converts inactive channels into active ones. Both proteolytically cleaved (active) and uncleaved (inactive) channels are present at the cell surface. Here we found that Hrs selectively controls trafficking of proteolytically cleaved channels. Expression of Hrs-ΔUIM dramatically slowed degradation of the cell surface pool of cleaved channels but not the surface pool of uncleaved channels. This observation is interesting because it provides evidence that proteolytically cleaved and uncleaved channels are trafficked differently within the endocytic pathway. In addition, it indicates that some membrane proteins are degraded through a mechanism independent of the Hrs UIM. The reason for this difference in degradation of cleaved and uncleaved channels is unclear. We found that both forms of αENaC coprecipitated with Hrs (Fig. 1*A*), indicating that both are delivered to the compartment where Hrs resides and that both bind to Hrs. Other parts of the ESCRT-0 complex are known to interact with ubiquitin, including the UIM of STAM and the Vps-27, Hrs, and STAM (VHS) domains of both Hrs and STAM (20, 21). Thus, the cleaved ENaC might be specifically reliant on recognition by the Hrs UIM, whereas other cargo, such as the uncleaved ENaC, might be recognized and sorted efficiently by other UIMs that reside in ESCRT-0.

In previous work, we found that the kinases SGK and PKA reduce ENaC endocytosis by inhibiting its binding of Nedd4-2 (12, 14). As a result, these kinases and their upstream activators (aldosterone and vasopressin, respectively) increase ENaC surface expression, and hence, epithelial Na^+ absorption. cAMP (presumably via PKA) also increased ENaC surface expression through enhanced recycling (42). Our current work provides a potential mechanism by which PKA (cAMP) and SGK could increase ENaC recycling. We found that SGK and cAMP reduced ENaC binding to Hrs. By decreasing ENaC sorting to lysosomes, this would increase the pool of ENaC available to recycle to the cell surface.

The regulation of epithelial Na^+ absorption is critical to maintain Na^+ homeostasis and to control blood pressure. Defects in Na^+ transport cause hypertension and lung diseases including cystic fibrosis. Our data suggest that the delivery of ENaC to the ESCRT machinery is a critical step in controlling Na^+ transport. Mutations that cause inherited hypertension (Liddle syndrome) reduced ENaC binding to Hrs, as did signaling pathways critical for the regulation of Na^+ transport. Thus, discovery of additional pathways that regulate ENaC binding to Hrs and identification of additional ESCRT proteins that modulate ENaC trafficking will provide new insight into mechanisms that regulate epithelial Na^+ absorption.

Acknowledgments—We thank Caitlin Digman and Zeru Peterson for assistance and acknowledge the University of Iowa DNA Core Facility for sequencing and reagents.

REFERENCES

1. Schild, L. (2004) *Rev. Physiol. Biochem. Pharmacol.* **151,** 93–107
2. Snyder, P. M. (2005) *Endocrinology* **146,** 5079–5085
3. Lifton, R. P. (1996) *Science* **272,** 676–680
4. Boucher, R. C., Stutts, M. J., Knowles, M. R., Cantley, L., and Gatzy, J. T. (1986) *J. Clin. Invest.* **78,** 1245–1252
5. Snyder, P. M. (2009) *Sci. Signal.* **2,** pe41
6. Zhou, R., Patel, S. V., and Snyder, P. M. (2007) *J. Biol. Chem.* **282,** 20207–20212
7. Staub, O., Dho, S., Henry, P., Correa, J., Ishikawa, T., McGlade, J., and Rotin, D. (1996) *EMBO J.* **15,** 2371–2380
8. Snyder, P. M., Olson, D. R., McDonald, F. J., and Bucher, D. B. (2001) *J. Biol. Chem.* **276,** 28321–28326
9. Snyder, P. M., Price, M. P., McDonald, F. J., Adams, C. M., Volk, K. A., Zeiher, B. G., Stokes, J. B., and Welsh, M. J. (1995) *Cell* **83,** 969–978
10. Firsov, D., Schild, L., Gautschi, I., Mérillat, A. M., Schneeberger, E., and Rossier, B. C. (1996) *Proc. Natl. Acad. Sci. U.S.A.* **93,** 15370–15375
11. Knight, K. K., Olson, D. R., Zhou, R., and Snyder, P. M. (2006) *Proc. Natl. Acad. Sci. U.S.A.* **103,** 2805–2808
12. Snyder, P. M., Olson, D. R., and Thomas, B. C. (2002) *J. Biol. Chem.* **277,** 5–8
13. Debonneville, C., Flores, S. Y., Kamynina, E., Plant, P. J., Tauxe, C., Thomas, M. A., Münster, C., Chraïbi, A., Pratt, J. H., Horisberger, J. D., Pearce, D., Loffing, J., and Staub, O. (2001) *EMBO J.* **20,** 7052–7059
14. Snyder, P. M., Olson, D. R., Kabra, R., Zhou, R., and Steines, J. C. (2004) *J. Biol. Chem.* **279,** 45753–45758
15. Soundararajan, R., Zhang, T. T., Wang, J., Vandewalle, A., and Pearce, D. (2005) *J. Biol. Chem.* **280,** 39970–39981
16. Kabra, R., Knight, K. K., Zhou, R., and Snyder, P. M. (2008) *J. Biol. Chem.* **283,** 6033–6039
17. Wang, H., Traub, L. M., Weixel, K. M., Hawryluk, M. J., Shah, N., Edinger, R. S., Perry, C. J., Kester, L., Butterworth, M. B., Peters, K. W., Kleyman, T. R., Frizzell, R. A., and Johnson, J. P. (2006) *J. Biol. Chem.* **281,** 14129–14135
18. Lu, C., Pribanic, S., Debonneville, A., Jiang, C., and Rotin, D. (2007) *Traffic* **8,** 1246–1264
19. Deleted in proof
20. Piper, R. C., and Luzio, J. P. (2007) *Curr. Opin. Cell Biol.* **19,** 459–465
21. Raiborg, C., and Stenmark, H. (2009) *Nature* **458,** 445–452
22. Piper, R. C., Cooper, A. A., Yang, H., and Stevens, T. H. (1995) *J. Cell Biol.* **131,** 603–617
23. Bilodeau, P. S., Urbanowski, J. L., Winistorfer, S. C., and Piper, R. C. (2002) *Nat. Cell Biol.* **4,** 534–539
24. Raiborg, C., Bremnes, B., Mehlum, A., Gillooly, D. J., D'Arrigo, A., Stang, E., and Stenmark, H. (2001) *J. Cell Sci.* **114,** 2255–2263
25. Hirano, S., Kawasaki, M., Ura, H., Kato, R., Raiborg, C., Stenmark, H., and Wakatsuki, S. (2006) *Nat. Struct. Mol. Biol.* **13,** 272–277
26. Mizuno, E., Kawahata, K., Kato, M., Kitamura, N., and Komada, M. (2003) *Mol. Biol. Cell* **14,** 3675–3689

27. Stern, K. A., Visser Smit, G. D., Place, T. L., Winistorfer, S., Piper, R. C., and Lill, N. L. (2007) *Mol. Cell. Biol.* **27,** 888–898
28. Marchese, A., Raiborg, C., Santini, F., Keen, J. H., Stenmark, H., and Benovic, J. L. (2003) *Dev. Cell* **5,** 709–722
29. Shih, S. C., Prag, G., Francis, S. A., Sutanto, M. A., Hurley, J. H., and Hicke, L. (2003) *EMBO J.* **22,** 1273–1281
30. McDonald, F. J., Snyder, P. M., McCray, P. B., Jr., and Welsh, M. J. (1994) *Am. J. Physiol.* **266,** L728–L734
31. McDonald, F. J., Price, M. P., Snyder, P. M., and Welsh, M. J. (1995) *Am. J. Physiol.* **268,** C1157–C1163
32. Snyder, P. M. (2000) *J. Clin. Invest.* **105,** 45–53
33. Chen, S. Y., Bhargava, A., Mastroberardino, L., Meijer, O. C., Wang, J., Buse, P., Firestone, G. L., Verrey, F., and Pearce, D. (1999) *Proc. Natl. Acad. Sci. U.S.A.* **96,** 2514–2519
34. Náray-Fejes-Tóth, A., Canessa, C., Cleaveland, E. S., Aldrich, G., and Fejes-Tóth, G. (1999) *J. Biol. Chem.* **274,** 16973–16978
35. Garty, H., and Palmer, L. G. (1997) *Physiol. Rev.* **77,** 359–396
36. Urbé, S., Sachse, M., Row, P. E., Preisinger, C., Barr, F. A., Strous, G., Klumperman, J., and Clague, M. J. (2003) *J. Cell Sci.* **116,** 4169–4179
37. Snyder, P. M., Olson, D. R., and Bucher, D. B. (1999) *J. Biol. Chem.* **274,** 28484–28490
38. Malik, R., and Marchese, A. (2010) *Mol. Biol. Cell* **21,** 2529–2541
39. Léon, S., Erpapazoglou, Z., and Haguenauer-Tsapis, R. (2008) *Mol. Biol. Cell* **19,** 2379–2388
40. Ren, J., Kee, Y., Huibregtse, J. M., and Piper, R. C. (2007) *Mol. Biol. Cell* **18,** 324–335
41. Lin, C. H., MacGurn, J. A., Chu, T., Stefan, C. J., and Emr, S. D. (2008) *Cell* **135,** 714–725
42. Butterworth, M. B., Edinger, R. S., Johnson, J. P., and Frizzell, R. A. (2005) *J. Gen. Physiol.* **125,** 81–101